Heliyon 9 (2023) e20619

Contents lists available at ScienceDirect

Heliyon

journal homepage: www.cell.com/heliyon

Research article

Tuneable Schottky contact of $MoSi_2N_4/TaS_2$ van der Waals heterostructure

Jinglin Xia, Yixiao Gu, Jun Mai, Tianyang Hu, Qikun Wang, Chao Xie, Yunkai Wu, Xu Wang *

Key Laboratory of Electronic Composites of Guizhou Province, College of Big Data and Information Engineering, Guizhou University, Guiyang 550025, Guizhou, People's Republic of China

A B S T R A C T

The two-dimensional $MoSi_2N_4$ monolayer is an emerging semiconductor material that offers considerable promise due to its ultra-thin profile, tuneable mechanical properties, excellent optoelectronic properties and exceptional environmental stability. The van der Waals (vdW) heterostructure formed by stacking such two-dimensional monolayers has demonstrated superior performance across various domains. In this study, a vdW heterostructure combining the two-dimensional $MoSi_2N_4$ and TaS_2 monolayers is examined using first-principles density functional theory. In its ground state, this van der Waals heterostructure establishes an ohmic contact with an exceptionally low potential barrier height. By modulating the vdW heterostructure with an applied electric field of -0.1 V/Å and under vertical stress, we discovered that $MoSi_2N_4$ and TaS_2 can transition from an ohmic contact to a p-type Schottky with an ultra-low Schottky barrier height (SBH). Our observations may give valuable insights for designing reconfigurable, tuneable Schottky nano-devices with enhanced electronic and optical properties based on $MoSi_2N_4/TaS_2$.

1. Introduction

After the discovery of graphene as a two-dimensional material [1], its exceptional physical properties, such as high electron mobility [2], the quantum Hall effect [3] and the Dirac cone [4] have garnered significant attention [5–8]. However, the absence of an electronic band gap in graphene has limited its application in a wide range of fields. Mang newer two-dimensional materials [9] discovered based on graphene have direct semiconducting properties. The atomic-level thickness [10], excellent optoelectronic [11] and mechanical properties [12] of these two-dimensional materials has drawn considerable interest from both the scientific and industrial communities. However, much like graphene, these new 2D materials have their limitations. For instance, the low carrier mobility [13] of MoS_2 limits its use in optoelectronics and nano-electronics. Finding a solution strategy for 2D materials remains challenging. Current researchers are keen to explore more practical applications in optoelectronics, nano-electronics and semiconductors. A promising solution is building van der Waals heterostructures (vdw) by combining two or more different materials in two dimensions. This approach not only combines the benefits of two-dimensional materials but also introduces unusual physics, excellent optical properties, and many new phenomena [14–17]. Recent investigations have delved deeply into single-to-multilayer 2D materials and their vertically stacked van der Waals heterostructures, which boast tuneable electronic properties and extraordinary mechanical characteristics [18,19].

$MoSi_2N_4$ monolayer film is a new type of two-dimensional transition metal nitrides material [20]. This monolayer comprises a sevenfold atomic layer sequence of N-Si-N-Mo-N-Si-N. It can be visualised as two Si-N bilayers sandwiching a single MoN_2 layer. The two-dimensional layered $MoSi_2N_4$ possesses robust mechanical strength and stability in air. Its intrinsic electron and hole mobili-

* Corresponding author.
E-mail address: xuwang@gzu.edu.cn (X. Wang).

https://doi.org/10.1016/j.heliyon.2023.e20619
Received 7 August 2023; Received in revised form 2 October 2023; Accepted 2 October 2023

Available online 5 October 2023

ties are $270cm^2V^{-1}s^{-1}$ and $1200cm^2V^{-1}s^{-1}$, respectively, which are approximately four times higher than MoS_2. The properties of the $MoSi_2N_4$ monolayer have been extensively studied. For instance, its adsorption of with different metal atoms reveals magnetic and electronic behaviours that suitable for spintronic nano-devices preparation [21]. Furthermore, the modulation of its electronic properties and the broadening of its applications can be achieved by doping organic molecules with $MoSi_2N_4$ [22]. Its non-magnetic semiconductor properties, high carrier mobility, robust mechanical strength and exceptional environmental stability hold potential for innovative applications [23–28]. Following the success of graphene, a new type of non-graphene-based 2D material, transition metal disulfides (TMDC), has emerged as a promising component for electronic and optoelectronic devices [9,29,30], TMDC [31], a 2D material, has been widely researched recently. Unlike traditional semiconductors, 2D layered semiconductor materials show promise in areas such as nano-electronic devices and optoelectronics due to their ultra-thin thickness, unique energy band structure, semiconducting or superconducting properties and remarkable mechanical characteristics [32]. Tantalum disulfide (TaS_2), a TMDC family member, functions as a vdW conductor at room temperature but transforms into a superconductor at extremely low temperatures [33,34]. Its superconductivity [35], charge density wave (CDW) [36], and cepstrum properties [37] have attracted considerable attention. TaS_2 crystals have stacked layers wherein the transition metal atomic sheets are positioned between sulfur atomic sheets in an S-Ta-S sequence. The chemical bonding within these layers is covalent, and the individual layers are connected by vdW interactions, allowing for intercalation between layers and facilitating exfoliation [33,38,39]. Although there has been significant research on heterostructures constructed from $MoSi_2N_4$ [40–42], the semiconductor contact formed by building heterostructures with metals remains underdeveloped.

When a metallic 2D material contacts a semiconductor 2D material, forming a heterostructures, it typically creates a Schottky barrier [43–45]. In this study, we constructed vdw heterostructures composed of $MoSi_2N_4$ and TaS_2 for the first time and computed their properties using first-principles based on density functional theory. We focused on understanding the regularity of the energy band structure and studied its Schottky properties under an applied electric field and vertical strain. Our findings show that the contact within the heterostructure can transition from an ohmic contact to a p-type Schottky contact by modulating the applied electric field and vertical deformation. Our research offers theoretical insight into novel Schottky heterostructures and provides theoretical guidance for their potential applications in optoelectronic devices as well as semiconductor devices.

2. Computational details

The calculations in this study were implemented using the Vienna ab initio Simulation Package. Electron-ion interactions were assessed via the projector-augmented wave potentials method [46], Structural optimisation, along with calculation of the electronic and physical properties of the monolayer $MoSi_2N_4$ and monolayer TaS_2 vertically contacted heterostructure, were conducted using density functional theory (DFT) [47]. For exchange-associative generalised functions, the generalised gradient approximation in the Perdew Burke Ernzerhof form was employed [48]. A kinetic energy cutoff of 520 eV was chosen for the plane wave basis set across all calculations. The first Brillouin zone of this system adopted a 7 x 7 x 1 Monkhorst Pack k-point grid for comprehensive geometric optimisation. The convergence threshold for the energy of the system was set at 1.0×10^{-7} eV, while the criterion for atomic force convergence was 0.01 eV/Å. Interlayer vdW interactions were described using DFT-D3 [49], with a vacuum layer exceeding 20 Å along the z-axis of the heterostructure to minimise vdW interactions between adjacent layers.

The geometric and electronic structures of monolayer $MoSi_2N_4$ and TaS_2 were initially analysed to accurately calculate the heterostructure. The optimised lattice constants for $MoSi_2N_4$ monolayers were a = b = 2.91 Å, while those for TaS_2 monolayers were a = b = 3.34 Å. These findings align with previously reported lattice constants [50,51]. Figs. 1(a) and 1(b) present the top and side views of $MoSi_2N_4$, and the Bader charges of the two-dimensional monolayer $MoSi_2N_4$ are shown in Fig. 1(b). The Mo atoms lost about 1.48 electrons, the N atoms in the top and bottom layers gained about 2.22 electrons, and the N atoms in the middle sandwich gained 1.48 charges. Each Si atom lost 2.96 charges. These charges redistribution differences mainly stem from the atomic structure of the material and the electronegativity differences between the elements. The Bader charges analysis reveals the distribution and rearrangement of electrons in a 2D monolayer of $MoSi_2N_4$, which is valuable for understanding the electronic properties of the material. The energy band structure of $MoSi_2N_4$ was also computed, revealing an indirect band gap of 1.78 eV for the monolayer, as shown in Fig. 1(c). This is consistent earlier studies [50]. A side view and top view of the single layer TaS_2 and the energy band diagram are shown in Figs. 1(d), 1(e) and 1(f) respectively.

3. Result and discussion

The lattice mismatch rate of a heterostructure is a crucial factor in its construction. In general, the lattice mismatch ratio is defined as the ratio of the absolute value of the difference between the lattice constants of two materials to the average value of their lattice constants. By constructing supercells, the lattice mismatch rate of a heterostructure can be significantly reduced. For this purpose, we used a 2×2 $MoSi_2N_4$ supercell and a $\sqrt{3} \times \sqrt{3}$ TaS_2 supercell to construct the heterostructure. As demonstrated in the Figs. 2(a) and (b), the lattice mismatch of the formed heterostructure is a mere 0.317%. This exceptionally low lattice mismatch rate suggests that the $MoSi_2N_4/TaS_2$ heterostructure is stably constructed. After structural optimisation, the layer spacing of $MoSi_2N_4/TaS_2$ measures 3.212 Å. Notably, this layer spacing is comparable to that of other typical $MoSi_2N_4$ heterostructures [52–54].

To verify the stability of the heterostructure, we further calculated the binding energy E_b, of the vdW heterostructure at the optimal layer spacing. This which can be obtained using the equation: $E_b = \left(E_T - E_{MoSi_2N_4} - E_{TaS_2}\right)/N$. Where $E_T, E_{MoSi_2N_4}, E_{TaS_2}$, and N denote the total energy of the heterostructure, the total energy of the $MoSi_2N_4$ monolayer, the total energy of the TaS_2

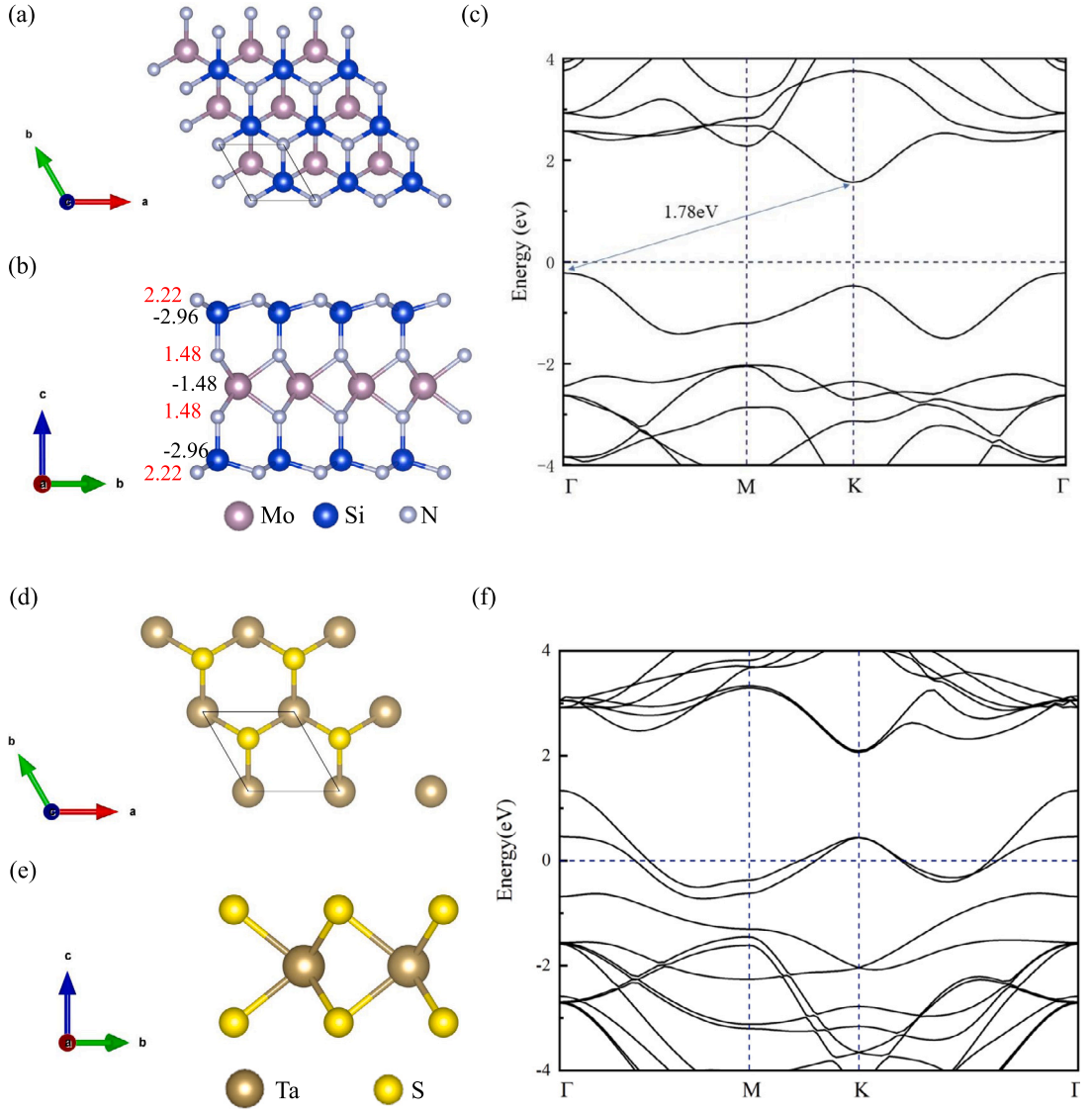

Fig. 1. (a) Top view and (b) side view of the monolayer $MoSi_2N_4$. (c) Band structure of $MoSi_2N_4$. (d) Top view and (e) side view of the monolayer TaS_2. (f) Band structure of TaS_2.

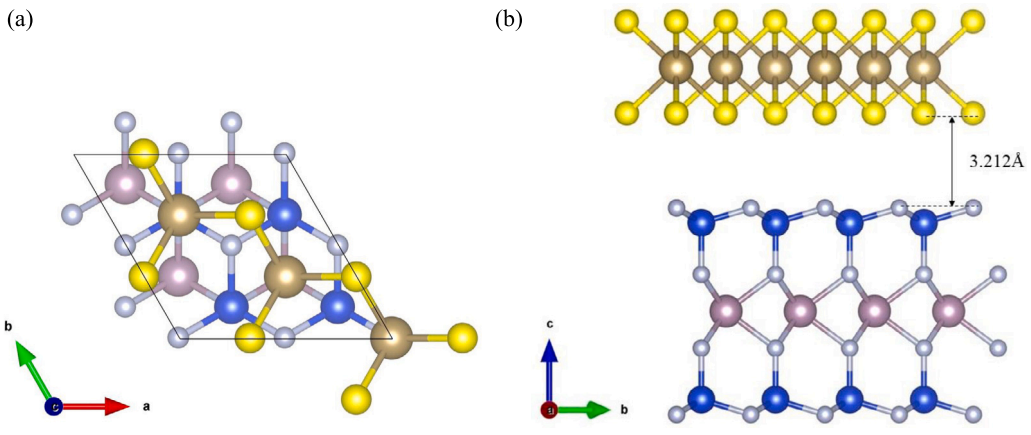

Fig. 2. Atomic structure of (a) Top view and (b) side view of the $MoSi_2N_4$ and TaS_2 heterostructure.

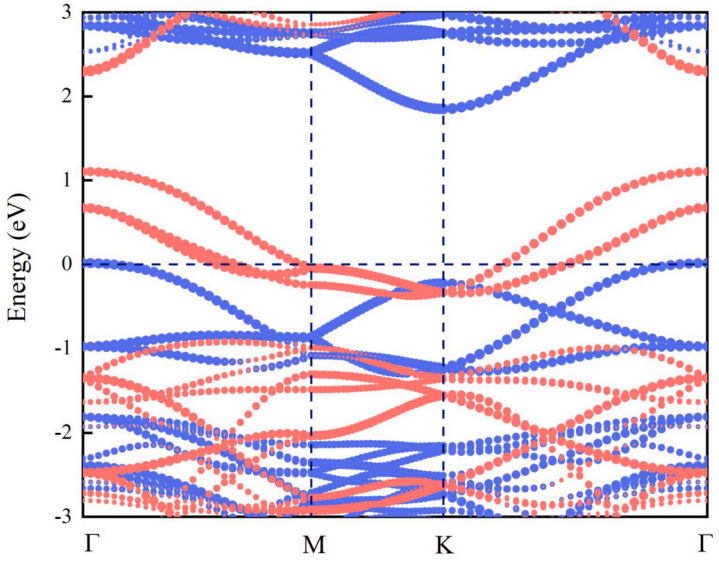

Fig. 3. The projected electronic band structures of $MoSi_2N_4$ and TaS_2. Here, blue and red symbols denote the contributions from $MoSi_2N_4$ and TaS_2, respectively.

monolayer and the number of atoms in the heterostructure, respectively. The calculated E_b is -0.176 eV/atom. A negative E_b suggests that the system releases energy during the formation of the heterostructure, implying that $MoSi_2N_4/TaS_2$ is stable. Because both $MoSi_2N_4$ and TaS_2 have excellent mechanical properties [26,38], the heterostructure is energetically stable and suitable for subsequent calculations.

When two monolayers are stacked vertically to form a heterogeneous structure, their properties are analysed by studying the projected energy band diagram, This can be viewed as a simple superposition of the two monolayers due to weak interlayer vdW interactions. The $MoSi_2N_4/TaS_2$ structure exhibits a clear metal/semiconductor vdW property. The projected energy bands of its ground state are depicted in Fig. 3. An indirect band gap is observed in the $MoSi_2N_4/TaS_2$ heterostructure due to energy band folding, a characteristic typical of two-dimensional VDWH [55]. In its ground state, the heterostructure presents an ohmic contact with ϕ_p of -0.007 eV. This extremely low ϕ_p allows the achievement of Schottky contacts between the heterostructure upon certain modulations. The SBH is determined via the Schottky-Mott rule [56,57], where $\phi_n = E_{CBM} - E_F$, $\phi_p = E_F - E_{VBM}$. Here, ϕ_n and ϕ_p denote the barrier heights of the interface potentials for electrons and holes respectively.

From an application perspective, the contact type and SBH of the $MoSi_2N_4/TaS_2$ vdW heterostructure are pivotal indicators of device performance. To valuate the feasibility and efficacy of $MoSi_2N_4/TaS_2$ vdW in advanced nano-device design, we also examined the regulation of heterostructure contact type and SBH through applied electric fields and interlayer coupling. Previously, for heterostructures such as Graphene/WSe_2 [58], Silicene/Janus Ga_2STe [59]and blue phosphorene/graphene, blue phosphorene/graphene-like gallium nitride [60], it has been shown that their electronic properties can be modulated by applying an applied electric field as well as by interlayer coupling. An external electric field is applied along the z-axis of the heterostructure, considering the direction from the $MoSi_2N_4$ layer to the TaS_2 layer as the positive direction of the electric field strength. The effect of the projected energy band structure, contact, type and SBH under varying electric fields is illustrated in Figs. 4(a), 4(b) and 4(c). With the applied electric field, and VBM and CBM of $MoSi_2N_4$ shift slightly in relation to the Fermi energy level. At an electric field of -0.1 V/Å, the $MoSi_2N_4/TaS_2$ contact type transitions from an ohmic contact to a p-type Schottky contact, with SBH (ϕ_p) and SBH (ϕ_n) being 0.021 eV and 1.819 eV, respectively. As the intensity of the negative electric field is increases, ϕ_p increases linearly while ϕ_n decreases correspondingly. When the negative electric field is less than -0.1 V/Å, the contact type of the heterostructure stabilises as Schottky p-type, Conversely, with a positive applied electric field, the contact type of the heterostructure stabilises as an ohmic contact. This shift in contact type is attributed to the Fermi energy level's change. Consequently, by adjusting the applied electric field, we can dynamically control the type of contact of the heterostructure. The ability to toggle between positive and negative electric fields permits free switching between ohmic and Schottky p-type contacts, a feature beneficial for electronic device design.

Interlayer coupling in heterostructure is an efficient method for tuning the electronic properties and SBH of vdW heterostructure. The layer spacing between vdWH can be modified by nano-mechanical pressure [61], vacuum annealing [62], and insertion of hexagonal BN dielectric layers [63] or diamond [64]. We examined the structural changes in the energy band of the heterostructure under vertical strain and the transformation of the contact type. We observed that when the layer spacing of the heterostructure was adjusted, it reduced to 2.612 Å, resulting in ultra-low p-type Schottky contacts. The n-type SBH (ϕ_p) and p-type SBH (ϕ_n) are 0.005 eV and 1.808 eV, respectively. An ultra-low p-type SBH suggests that TaS_2 serves as an efficient two-dimensional electrical contact for $MoSi_2N_4$ under certain conditions. To further investigate the effect of layer spacing on the heterostructure, we computed the energy band structure of vdWH at varying layer spacings, as shown in Figs. 5(a), 5(b) and 5(c). We determined that applying vertical strain caused a shift in the Fermi energy level of the TaS_2 layer. Specifically, when the layer spacing was reduced from 3.212 Å to 2.212 Å, the Fermi energy level of the TaS_2 layer shifted towards the CBM of the semiconductor. This shift transitioned the vdWH from

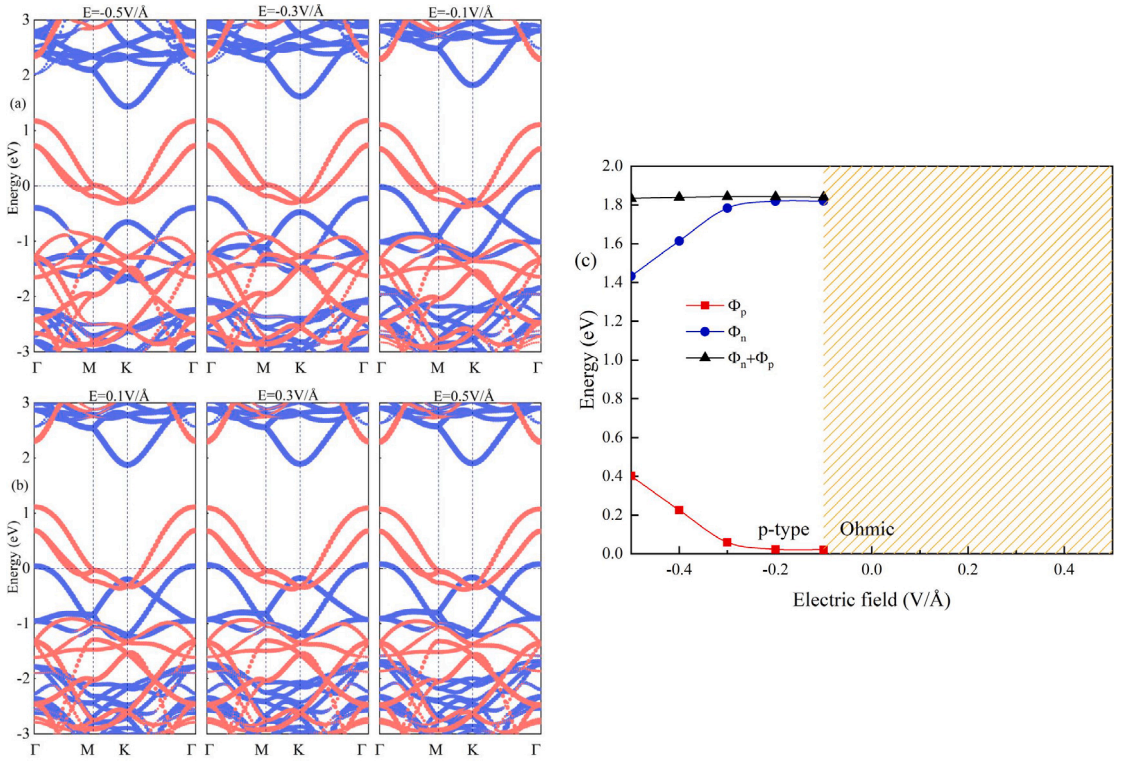

Fig. 4. Projected band structures of the $MoSi_2N_4/TaS_2$ heterostructure under negative electric gating of (a) and positive electric gating of (b). Here, blue and red symbols denote the contributions from $MoSi_2N_4$ and TaS_2, respectively. (c) The variations of SBH as a function of electric gating.

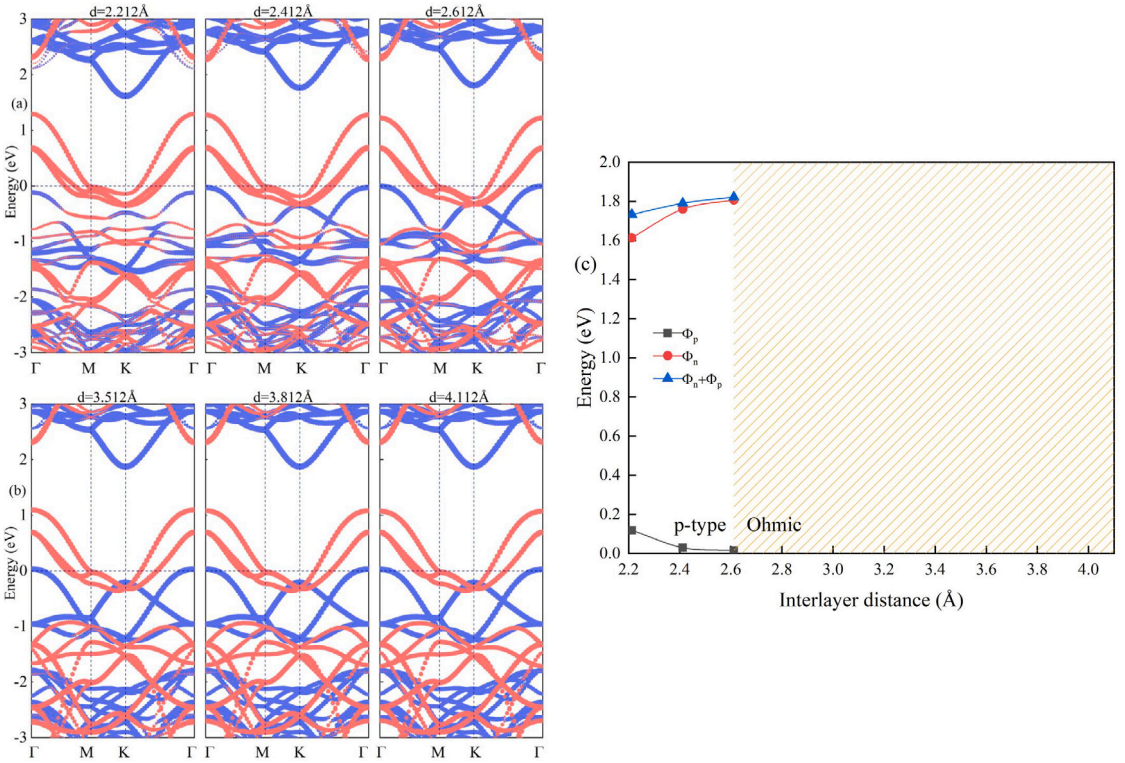

Fig. 5. Projected band structures of the $MoSi_2N_4/TaS_2$ heterostructure under (a) compressive and (b) tensile strains. Here, blue and red symbols denote the contributions from $MoSi_2N_4$ and TaS_2, respectively. (c) The variations of SBH as a function of interlayer spacing.

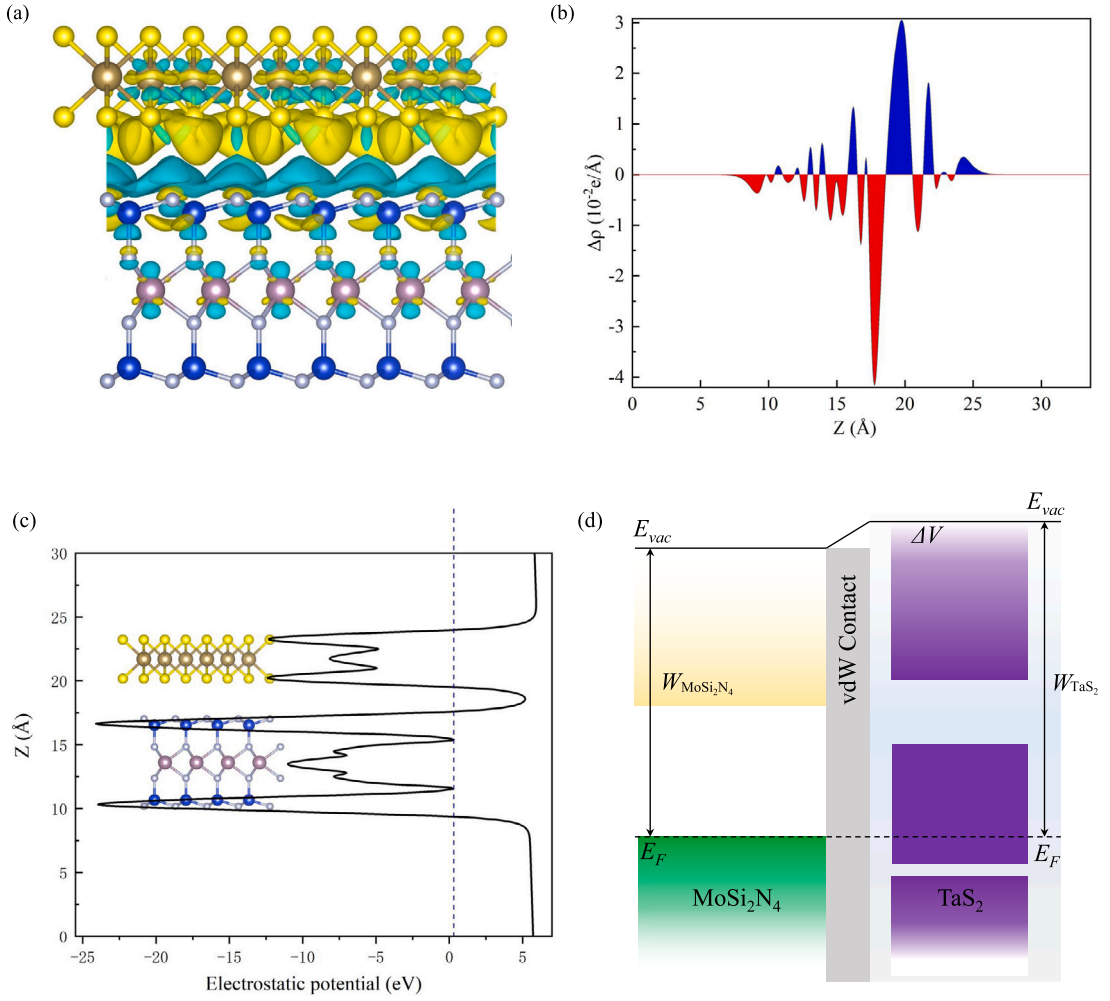

Fig. 6. (a) Charge density difference of the $MoSi_2N_4/TaS_2$ VHT. Yellow and cyan regions represent charge accumulation and depletion, respectively. (b) Plane-averaged differential charge density $\Delta\rho$. (c) planar average electrostatic potential differences. (d) band alignment of $MoSi_2N_4/TaS_2$ heterostructure.

an ohmic to a p-type Schottky contact. Conversely, when the layer spacing exceeded 2.612 Å, the Fermi level migrated towards the VBM of the semiconductor and a transition of the interface contact from p-type Schottky to ohmic was noticeable. Heterostructures, whether modulated by an applied electric field or interlayer coupling, exhibit ultra-low p-type SBH. This ultra-low p-type SBH boasts a high charge injection efficiency, making it particularly advantageous for nano-electronic devices.

This study further examined the three-dimensional charge density difference of $MoSi_2N_4/TaS_2$ along the z-axis to understand the redistribution of charge after constructing a heterogeneous structure of two-dimensional material. The three-dimensional charge density difference can be defined as follows: $\Delta\rho(z) = \rho(z) - \rho(z)_{MoSi_2N_4} - \rho(z)_{TaS_2}$, where $\rho(z)$, $\rho(z)_{MoSi_2N_4}$, and $\rho(z)_{TaS_2}$ represent the total charge densities of the heterostructure, isolated $MoSi_2N_4$, and isolated TaS_2, respectively. As illustrated in Fig. 6(a), when $MoSi_2N_4$ contacts TaS_2, there is a charge redistribution at the interface. The $MoSi_2N_4$ layer is enveloped in cyan, indicating charge depletion, while the TaS_2 layer is enveloped in yellow, signifying charge accumulation. This suggests that charge transfers from the $MoSi_2N_4$ layer to the TaS_2 layer. To further elaborate on this charge redistribution, the planar average charge density difference $\Delta\rho$ along the z-axis of the heterostructure, $\Delta\rho$ indicates a certain amount of charge transfer between heterogeneous structures, Fig. 6(b) reveals the electron transfer amount and behaviour between the heterostructure. A negative $\Delta\rho$ is observed near the $MoSi_2N_4$ surface and a positive $\Delta\rho$ near the TaS_2, clearly confirming the charge transfer from $MoSi_2N_4$ to TaS_2, with charge depleting on the $MoSi_2N_4$ monolayer and accumulating on the TaS_2 monolayer. The charge transfer within the heterostructure generates an internal electron field, which effectively inhibits photoelectron and hole complexation. This extends the carrier lifetime in the $MoSi_2N_4/TaS_2$ heterostructure, and the charge transfer results in a Fermi energy level shift, leading to an ultra-low SBH. In addition, the planar average electrostatic potential of $MoSi_2N_4/TaS_2$ was computed, as shown in Fig. 6(c). The potential of $MoSi_2N_4$ is deeper than that of TaS_2. Finally, Fig. 6(d) presents the energy band alignment of the heterostructure.

In this study, we construct and investigate a $MoSi_2N_4/TaS_2$ heterostructure for the first time using first principles calculations. In its ground state, the contact heterostructure exhibits an ohmic contact. However, when modulated under an applied electric field

and vertical strain, the contact type transitions from ohmic to a p-type Schottky contact once the applied electric field reaches -0.1 V/Å and the layer spacing decreases to 2.612 Å. Adjusting the SBH through an electric field and interlayer distance and achieving a contact type switch offers valuable insights for enhancing nano-electronic devices. The $MoSi_2N_4/TaS_2$ heterostructure also boasts high carrier mobility, making it a promising candidate for high-speed nano-electronic applications. This study's findings guide designing tuneable Schottky nano-devices with superior electronic and optical attributes.

Author contribution statement

Jinglin Xia: Conceived and designed the experiments; Performed the experiments; Analyzed and interpreted the data; Wrote the paper.

Tianyang Hu; Qikun Wang and Jun Mai: Contributed reagents, materials, analysis tools or data.

Yixiao Gu and Chao Xie: Analyzed and interpreted the data.

Yunkai Wu and Xu Wang: Analyzed and interpreted the data; Contributed reagents, materials, analysis tools or data.

Xu Wang: Supervised the work.

CRediT authorship contribution statement

Jinglin Xia: Conceptualization, Data curation, Formal analysis, Investigation, Methodology, Project administration, Resources, Software, Validation, Visualization, Writing – original draft, Writing – review & editing. **Yixiao Gu:** Methodology. **Jun Mai:** Project administration. **Tianyang Hu:** Formal analysis. **Qikun Wang:** Investigation. **Chao Xie:** Software. **Yunkai Wu:** Validation. **Xu Wang:** Investigation.

Declaration of competing interest

The authors declare that they have no known competing financial interests or personal relationships that could have appeared to influence the work reported in this paper.

Data availability

Data included in article/supp. material/referenced in article.

Acknowledgements

This paper was supported by the Natural Science Platform Foundation of Guizhou Province, China, grant number ZCKJ [2021] 015, and the National Natural Science Foundation of China (No. 52262020).

References

[1] K.S. Novoselov, A.K. Geim, S.V. Morozov, D.-e. Jiang, Y. Zhang, S.V. Dubonos, I.V. Grigorieva, A.A. Firsov, Electric field effect in atomically thin carbon films, Science 306 (2004) 666.

[2] Z. Liu, Z. Chen, C. Wang, H.I. Wang, M. Wuttke, X.-Y. Wang, M. Bonn, L. Chi, A. Narita, K. Müllen, Bottom-up, on-surface-synthesized armchair graphene nanoribbons for ultra-high-power micro-supercapacitors, J. Am. Chem. Soc. 142 (2020) 17881.

[3] A.R. Panna, I.-F. Hu, M. Kruskopf, D.K. Patel, D.G. Jarrett, C.-I. Liu, S.U. Payagala, D. Saha, A.F. Rigosi, D.B. Newell, et al., Graphene quantum Hall effect parallel resistance arrays, Phys. Rev. B 103 (2021) 075408.

[4] M. Milićević, G. Montambaux, T. Ozawa, O. Jamadi, B. Real, I. Sagnes, A. Lemaître, L. Le Gratiet, A. Harouri, J. Bloch, et al., Type-iii and tilted Dirac cones emerging from flat bands in photonic orbital graphene, Phys. Rev. X 9 (2019) 031010.

[5] A.K. Geim, K.S. Novoselov, The rise of graphene, Nat. Mater. 6 (2007) 183.

[6] F. Schwierz, Graphene transistors, Nat. Nanotechnol. 5 (2010) 487.

[7] L. Cui, J. Wang, M. Sun, Graphene plasmon for optoelectronics, Rev. Phys. 6 (2021) 100054.

[8] J. Du, B. Tong, S. Yuan, N. Dai, R. Liu, D. Zhang, H.-M. Cheng, W. Ren, Advances in flexible optoelectronics based on chemical vapor deposition-grown graphene, Adv. Funct. Mater. 32 (2022) 2203115.

[9] S.Z. Butler, S.M. Hollen, L. Cao, Y. Cui, J.A. Gupta, H.R. Gutiérrez, T.F. Heinz, S.S. Hong, J. Huang, A.F. Ismach, et al., Progress, challenges, and opportunities in two-dimensional materials beyond graphene, ACS Nano 7 (2013) 2898.

[10] C. Soldano, A. Mahmood, E. Dujardin, Production, properties and potential of graphene, Carbon 48 (2010) 2127.

[11] C. Liu, H. Chen, S. Wang, Q. Liu, Y.-G. Jiang, D.W. Zhang, M. Liu, P. Zhou, Two-dimensional materials for next-generation computing technologies, Nat. Nanotechnol. 15 (2020) 545.

[12] C. Lee, X. Wei, J.W. Kysar, J. Hone, Measurement of the elastic properties and intrinsic strength of monolayer graphene, Science 321 (2008) 385.

[13] B. Radisavljevic, A. Radenovic, J. Brivio, V. Giacometti, A. Kis, Single-layer MoS2 transistors, Nat. Nanotechnol. 6 (2011) 147.

[14] K. Guo, X. Wang, R. Zhang, Z. Fu, L. Zhang, G. Ma, C. Deng, Multiferroic oxide BFCNT/BFCO heterojunction black silicon photovoltaic devices, Light: Sci. Appl. 10 (2021) 201.

[15] J. Chen, G. Ma, B. Gong, C. Deng, M. Zhang, K. Guo, R. Cui, Y. Wu, M. Lv, X. Wang, Bulk photovoltaic current mechanisms in all-inorganic perovskite multiferroic materials, Nanomaterials 13 (2023) 429.

[16] H. Din, M. Idrees, A. Albar, M. Shafiq, I. Ahmad, C.V. Nguyen, B. Amin, Rashba spin splitting and photocatalytic properties of GeC-MSSe (m = Mo, w) van der Waals heterostructures, Phys. Rev. B 100 (2019) 165425.

[17] D. Pierucci, H. Henck, J. Avila, A. Balan, C.H. Naylor, G. Patriarche, Y.J. Dappe, M.G. Silly, F. Sirotti, A.C. Johnson, et al., Band alignment and minigaps in monolayer MoS2-graphene van der Waals heterostructures, Nano Lett. 16 (2016) 4054.

[18] M.R. Islam, M.S. Islam, M.Y. Zamil, N. Ferdous, C. Stampfl, J. Park, M.K. Hossain, Two-dimensional BAs/GeC van der Waals heterostructures: a widely tunable photocatalyst for water splitting and hydrogen production, J. Phys. Chem. Solids 176 (2023) 111263.
[19] H. Guo, X. Lang, X. Tian, W. Jiang, G. Wang, Tunable Schottky barrier in Janus-XGa2 Y/Graphene (X/Y= S, Se, Te; X≠ Y) van der Waals heterostructures, Nanotechnology 33 (2022) 425704.
[20] Y.-L. Hong, Z. Liu, L. Wang, T. Zhou, W. Ma, C. Xu, S. Feng, L. Chen, M.-L. Chen, D.-M. Sun, et al., Chemical vapor deposition of layered two-dimensional MoSi2N4 materials, Science 369 (2020) 670.
[21] Z. Cui, K. Yang, K. Ren, S. Zhang, L. Wang, Adsorption of metal atoms on MoSi2N4 monolayer: a first principles study, Mater. Sci. Semicond. Process. 152 (2022) 107072.
[22] Z. Cui, Y. Luo, J. Yu, Y. Xu, Tuning the electronic properties of MoSi2N4 by molecular doping: a first principles investigation, Physica E, Low-Dimens. Syst. Nanostruct. 134 (2021) 114873.
[23] M. Sun, M. Re Fiorentin, U. Schwingenschlögl, M. Palummo, Excitons and light-emission in semiconducting MoSi2X4 two-dimensional materials, npj 2D Mater. Appl. 6 (2022) 81.
[24] K. Ren, H. Shu, K. Wang, H. Qin, Two-dimensional MX 2 Y 4 systems: ultrahigh carrier transport and excellent hydrogen evolution reaction performances, Phys. Chem. Chem. Phys. 25 (2023) 4519.
[25] J. Yuan, Q. Wei, M. Sun, X. Yan, Y. Cai, L. Shen, U. Schwingenschlögl, et al., Protected valley states and generation of valley- and spin-polarized current in monolayer M A 2 Z 4, Phys. Rev. B 105 (2022) 195151.
[26] B. Mortazavi, B. Javvaji, F. Shojaei, T. Rabczuk, A.V. Shapeev, X. Zhuang, Exceptional piezoelectricity, high thermal conductivity and stiffness and promising photocatalysis in two-dimensional MoSi2N4 family confirmed by first-principles, Nano Energy 82 (2021) 105716.
[27] X.-S. Guo, S.-D. Guo, Tuning transport coefficients of monolayer MoSi2N4 with biaxial strain, Chin. Phys. B 30 (2021) 067102.
[28] Q. Peng, Z. Wang, B. Sa, B. Wu, Z. Sun, Electronic structures and enhanced optical properties of blue phosphorene/transition metal dichalcogenides van der Waals heterostructures, Sci. Rep. 6 (2016) 1.
[29] F. Wang, Z. Wang, Q. Wang, F. Wang, L. Yin, K. Xu, Y. Huang, J. He, Synthesis, properties and applications of 2D non-graphene materials, Nanotechnology 26 (2015) 292001.
[30] M. Xu, T. Liang, M. Shi, H. Chen, Graphene-like two-dimensional materials, Chem. Rev. 113 (2013) 3766.
[31] Q.H. Wang, K. Kalantar-Zadeh, A. Kis, J.N. Coleman, M.S. Strano, Electronics and optoelectronics of two-dimensional transition metal dichalcogenides, Nat. Nanotechnol. 7 (2012) 699.
[32] S. Manzeli, D. Ovchinnikov, D. Pasquier, O.V. Yazyev, A. Kis, 2D transition metal dichalcogenides, Nat. Rev. Mater. 2 (2017) 1.
[33] E. Navarro-Moratalla, J.O. Island, S. Manas-Valero, E. Pinilla-Cienfuegos, A. Castellanos-Gomez, J. Quereda, G. Rubio-Bollinger, L. Chirolli, J.A. Silva-Guillén, N. Agraït, et al., Enhanced superconductivity in atomically thin TaS2, Nat. Commun. 7 (2016) 11043.
[34] Q. Dong, J. Pan, S. Li, Y. Fang, T. Lin, S. Liu, B. Liu, Q. Li, F. Huang, B. Liu, Record-high superconductivity in transition metal dichalcogenides emerged in compressed 2H-TaS2, Adv. Mater. 34 (2022) 2103168.
[35] A.C. Neto, Charge density wave, superconductivity, and anomalous metallic behavior in 2D transition metal dichalcogenides, Phys. Rev. Lett. 86 (2001) 4382.
[36] I. Guillamón, H. Suderow, J.G. Rodrigo, S. Vieira, P. Rodiere, L. Cario, E. Navarro-Moratalla, C. Martí-Gastaldo, E. Coronado, Chiral charge order in the superconductor 2H-TaS2, New J. Phys. 13 (2011) 103020.
[37] L. Stojchevska, I. Vaskivskyi, T. Mertelj, P. Kusar, D. Svetin, S. Brazovskii, D. Mihailovic, Ultrafast switching to a stable hidden quantum state in an electronic crystal, Science 344 (2014) 177.
[38] Y. Yang, S. Fang, V. Fatemi, J. Ruhman, E. Navarro-Moratalla, K. Watanabe, T. Taniguchi, E. Kaxiras, P. Jarillo-Herrero, Enhanced superconductivity upon weakening of charge density wave transport in 2 H-TaS 2 in the two-dimensional limit, Phys. Rev. B 98 (2018) 035203.
[39] Y. Hu, Q. Hao, B. Zhu, B. Li, Z. Gao, Y. Wang, K. Tang, Toward exploring the structure of monolayer to few-layer TaS 2 by efficient ultrasound-free exfoliation, Nanoscale Res. Lett. 13 (2018) 1.
[40] J.Q. Ng, Q. Wu, L. Ang, Y.S. Ang, Tunable electronic properties and band alignments of MoSi2N4/GaN and MoSi2N4/ZnO van der Waals heterostructures, Appl. Phys. Lett. 120 (2022) 103101.
[41] C. Liu, Z. Wang, W. Xiong, H. Zhong, S. Yuan, Effect of vertical strain and in-plane biaxial strain on type-II MoSi2N4/Cs3Bi2I9 van der Waals heterostructure, J. Appl. Phys. 131 (2022) 163102.
[42] Q. Wang, L. Cao, S.-J. Liang, W. Wu, G. Wang, C.H. Lee, W.L. Ong, H.Y. Yang, L.K. Ang, S.A. Yang, et al., Efficient Ohmic contacts and built-in atomic sublayer protection in MoSi2N4 and WSi2N4 monolayers, npj 2D Mater. Appl. 5 (2021) 71.
[43] H.T. Nguyen, M.M. Obeid, A. Bafekry, M. Idrees, T.V. Vu, H.V. Phuc, N.N. Hieu, L.T. Hoa, B. Amin, C.V. Nguyen, Interfacial characteristics, Schottky contact, and optical performance of a graphene/Ga 2 S Se van der Waals heterostructure: strain engineering and electric field tunability, Phys. Rev. B 102 (2020) 075414.
[44] L. Cao, Y.S. Ang, Q. Wu, L. Ang, Janus PtSSe and graphene heterostructure with tunable Schottky barrier, Appl. Phys. Lett. 115 (2019) 241601.
[45] L. Cao, G. Zhou, Q. Wang, L. Ang, Y.S. Ang, Two-dimensional van der Waals electrical contact to monolayer MoSi2N4, Appl. Phys. Lett. 118 (2021) 013106.
[46] P.E. Blöchl, Projector augmented-wave method, Phys. Rev. B 50 (1994) 17953.
[47] G. Kresse, J. Hafner, Ab initio molecular-dynamics simulation of the liquid-metal–amorphous-semiconductor transition in germanium, Phys. Rev. B 49 (1994) 14251.
[48] J.P. Perdew, K. Burke, M. Ernzerhof, Generalized gradient approximation made simple, Phys. Rev. Lett. 77 (1996) 3865.
[49] S. Grimme, J. Antony, S. Ehrlich, H. Krieg, A consistent and accurate ab initio parametrization of density functional dispersion correction (DFT-D) for the 94 elements H-Pu, J. Chem. Phys. 132 (2010) 154104.
[50] A. Bafekry, M. Faraji, D.M. Hoat, M. Shahrokhi, M. Fadlallah, F. Shojaei, S. Feghhi, M. Ghergherehchi, D. Gogova, MoSi2N4 single-layer: a novel two-dimensional material with outstanding mechanical, thermal, electronic and optical properties, J. Phys. D, Appl. Phys. 54 (2021) 155303.
[51] Y. Ding, Y. Wang, J. Ni, L. Shi, S. Shi, W. Tang, First principles study of structural, vibrational and electronic properties of graphene-like MX2 (M= Mo, Nb, W, Ta; X= S, Se, Te) monolayers, Physica B, Condens. Matter 406 (2011) 2254.
[52] P. Zhao, Z.-Y. Jiang, J.-M. Zheng, Y.-M. Lin, A. Du, Theoretical study of a novel WSi2N4/MoSi2N4 heterostructure with ultrafast carrier transport, J. Phys. Chem. C 126 (2022) 11380.
[53] G. Yuan, Z. Cheng, Y. Cheng, W. Duan, H. Lv, Z. Liu, C. Han, X. Ma, Highly sensitive band alignment of the graphene/MoSi2N4 heterojunction via an external electric field, ACS Appl. Electron. Mater. 4 (2022) 2897.
[54] A. Bafekry, M. Faraji, A.A. Ziabari, M. Fadlallah, C.V. Nguyen, M. Ghergherehchi, S. Feghhi, A van der Waals heterostructure of MoS 2/MoSi 2 N 4: a first-principles study, New J. Chem. 45 (2021) 8291.
[55] X. Zhou, X. Hu, J. Yu, S. Liu, Z. Shu, Q. Zhang, H. Li, Y. Ma, H. Xu, T. Zhai, 2D layered material-based van der Waals heterostructures for optoelectronics, Adv. Funct. Mater. 28 (2018) 1706587.
[56] W. Schottky, Zur halbleitertheorie der sperrschicht-und spitzengleichrichter, Z. Phys. 113 (1939) 367.
[57] J. Bardeen, Surface states and rectification at a metal semi-conductor contact, Phys. Rev. 71 (1947) 717.
[58] M. Sun, J.-P. Chou, J. Yu, W. Tang, Effects of structural imperfection on the electronic properties of graphene/WSe 2 heterostructures, J. Mater. Chem. C 5 (2017) 10383.
[59] H. Shu, X. Liu, Interfacial electronic characteristics and tunable contact types in novel silicene/Janus Ga2STe heterobilayers, Surf. Interfac. 35 (2022) 102451.
[60] M. Sun, J.-P. Chou, J. Yu, W. Tang, Electronic properties of blue phosphorene/graphene and blue phosphorene/graphene-like gallium nitride heterostructures, Phys. Chem. Chem. Phys. 19 (2017) 17324.

[61] M. Dienwiebel, G.S. Verhoeven, N. Pradeep, J.W. Frenken, J.A. Heimberg, H.W. Zandbergen, Superlubricity of graphite, Phys. Rev. Lett. 92 (2004) 126101.
[62] S. Tongay, W. Fan, J. Kang, J. Park, U. Koldemir, J. Suh, D.S. Narang, K. Liu, J. Ji, J. Li, et al., Tuning interlayer coupling in large-area heterostructures with CVD-grown MoS2 and WS2 monolayers, Nano Lett. 14 (2014) 3185.
[63] H. Fang, C. Battaglia, C. Carraro, S. Nemsak, B. Ozdol, J.S. Kang, H.A. Bechtel, S.B. Desai, F. Kronast, A.A. Unal, et al., Strong interlayer coupling in van der Waals heterostructures built from single-layer chalcogenides, Proc. Natl. Acad. Sci. 111 (2014) 6198.
[64] S. Clark, K.-J. Jeon, J.-Y. Chen, C.-S. Yoo, Few-layer graphene under high pressure: Raman and X-ray diffraction studies, Solid State Commun. 154 (2013) 15.